

The Shortwave Reflectance of the Yankee Environmental Systems Hotplate

David Siuta, Jefferson R. Snider and Bujidmaa Borkhuu
University of Wyoming
September 2010
(Updated September 2017)

1 - Introduction

A Yankee Environmental Systems Hotplate Precipitation Sensor (hereafter the “hotplate”) is new type of precipitation gauge. Precipitation intensities reported by the hotplate are derived from measurement of the electrical power needed to maintain the hotplate’s upper surface at a constant temperature. Nominally, the plate surface temperature is set at 75 °C (Rasmussen et al., 2010). Other examples of heated constant-temperature meteorological sensors are the devices used to detect cloud water content (King et al., 1978; Korolev et al., 1998).

Assuming that the hotplate’s heat budget is at steady state, the electrical power supplied to its top plate can be equated to the rates of three heat transfer processes: 1) sensible heat transfer, 2) latent heat transfer (i.e., the component of the electrical power used to melt and evaporate precipitation), and 3) radiative heat transfer both at visible wavelengths (shortwave heating) and infrared wavelengths (longwave cooling). Typically, it is assumed that the net radiative heat transfer term is negligible. If that assumption is valid, then the electrical power minus the sensible heat term is proportional to the latent heat transfer and thus proportional to the precipitation intensity (Rasmussen et al., 2010). We show that this assumption can lead to substantial bias in a hotplate’s report of precipitation intensity ($\geq 10\%$). We also report measurements of the hotplate’s reflectance at solar (shortwave) wavelengths and show how the derived reflectance, combined measurement of solar irradiance, can be used to correct a hotplate’s biased report of precipitation intensity.

Figure 1 shows the top surface of the hotplate; we refer to this as the “sensor plate.” The sensor plate consists of a horizontal surface, diameter 0.13 m, and has three concentric rings extending vertically from its surface. Not seen in Figure 1 is the lower hotplate surface, here referred to as the “reference plate.” The reference plate is a mirror image of the sensor plate.



Figure 1 – The Yankee Environmental Systems Hotplate Precipitation Sensor (<http://www.yesinc.com/products/data/tps3100/index.html>).

A parameter used in this analysis is the surface area of the upper plate. Sensible heat energy is transported across an area equal to the sum of the plate’s horizontal surface area (0.013 m^2) plus the vertical surface area of the three rings (0.005 m^2). From the perspective of solar irradiance, the active surface area is approximately 0.002 m^2 smaller than the sum of horizontal and vertical areas. Throughout this analysis we approximate the effective hotplate surface area as the sum of horizontal and vertical areas ($A_{hp} = 0.018 \text{ m}^2$) and apply this surface area regardless of the specific process being analyzed (solar heating, sensible heating, etc.).

The hotplate microprocessor reports sensor data every second. Three of these measurements are used in this report: 1) the electrical power supplied to the sensor plate, 2) ambient temperature, and 3) wind speed. The latter is derived from values of ambient temperature and the electrical power supplied to the reference (bottom) plate (Rasmussen et al., 2010). Values of wind speed, and the ambient temperature, are used to derive the rate of sensible heat transfer from the sensor plate (Borkhuu, 2009). The derived sensible heat transfer rate is subtracted from the sensor plate electrical power and a power difference is formulated. An example of this is shown in Figure 2. The figure shows twelve hours of measurements made during operation of the hotplate on a 25 m tower located in the Medicine Bow Mountains of southeastern Wyoming. The Figures 2b-2c show the sensor plate electrical power and wind speed measurements; Figure 2a has measurements from collocated longwave and shortwave radiation sensors, and Figure 2d has the power difference (i.e., electrical power supplied to sensor plate minus the sensible heat transfer rate).

The twelve-hour interval shown in Figure 2 was free of both clouds and precipitation. This is evident from the smooth data traces in Figure 2a and from the amplitude of the daytime shortwave flux (local noon is at 18:00 UTC). To ease comparison of the radiative and hotplate data, Figure 2b presents the electrical power supplied to the sensor plate divided by A_{hp} ; this scaling converts the electrical power to an energy flux. The correlation seen between the electrical power (Figure 2b) and wind speed (Figure 2c) is an indication of the dominance of the sensible heat term in the plate's energy budget.

The departure from zero seen in Figure 2d has two important implications for the hotplate's measurement of precipitation. During daytime, when the hotplate is absorbing a fraction of the incident shortwave radiation, it is evident that the power difference is negative.

On days with precipitation, this negative difference (residual) leads to underestimation of the hotplate-reported precipitation intensity. Conversely, the positive difference during nighttime can alias as precipitation. The magnitude of the nighttime and daytime residuals - approximately 100 and 200 W m⁻² in Figure 2d - translate to a precipitation bias equal to 0.1 mm/hr (overestimate at night) and 0.2 mm/hr (underestimate during day). Because instantaneous wintertime precipitation intensities in southeastern Wyoming seldom exceed 2 mm/hr (Wolfe and Snider, 2010), these plus and minus residuals are indicative of significant (5% to 10%) uncertainty in determinations of wintertime precipitation reported by the hotplate.

This report documents simultaneous measurements of solar irradiance, with measurements of hotplate sensor plate power, wind speed and temperature. In our analysis we derive the hotplate's shortwave reflectance. Our measurements and analysis are described in the next section. In the summary, we compare our reflectance values to values for aluminum reported in the literature.

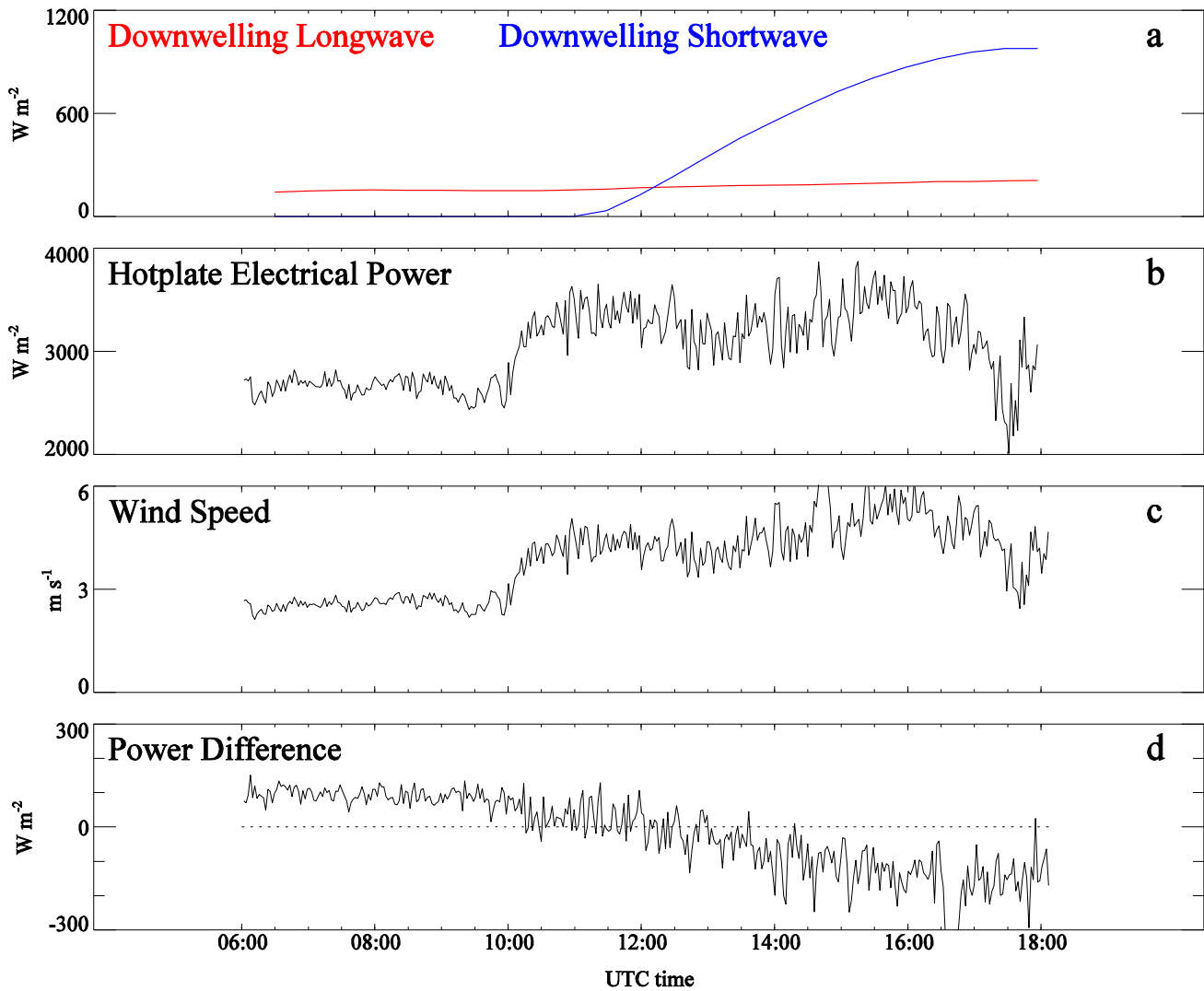


Figure 2 – (a) Time series of AmeriFlux downwelling longwave and shortwave radiation measurements, (b) electrical power supplied to the sensor plate divided by A_{hp} , (c) wind speed derived from electrical power supplied to the reference plate, temperature and wind speed, (d) difference between electrical power supplied to the sensor plate and the derived sensible heat transfer rate (Borkhuu, 2009), divided by A_{hp} . Measurements are from 20070414, acquired 25 m above ground level on the AmeriFlux tower located in the Medicine Bow Mountains of southeastern Wyoming.

2 - Measurements

Assuming steady state and no precipitation, and ignoring longwave radiative terms, the sensor plate's energy balance equation is

$$P = SH - A_{hp} \cdot I \cdot (1 - R), \quad (1)$$

where, P is the electrical power supplied to the sensor plate, SH is the sensor plate's sensible heat term (Borkhuu, 2009), I is the solar irradiance and R is the sensor plate's shortwave reflectance. In these experiments, the hotplate was either shaded from shortwave radiation, or illuminated by it. Equation 1 is formulated differently for the shaded and illuminated situations, here indicated by either a subscript "s" or "i", respectively:

$$P_i = SH_i - A_{hp} \cdot I \cdot (1 - R) \quad (2)$$

$$P_s = SH_s \quad (3)$$

Measurements of I , combined with hotplate measurements of P_i , P_s and derived values of SH_s and SH_i (Borkhuu, 2009), allow the reflectance to be calculated as

$$R = 1 - \frac{(P_s - P_i) - (SH_s - SH_i)}{I \cdot A_{hp}} \quad (4)$$

The direct normal component of the solar irradiance (I_N , W m^{-2}) was measured with an Eppley-Angstrom Compensation Pyrheliometer (Eppley Laboratory, 1976). During the experiments, paired measurements of I_N were obtained from the two channels of the pyrheliometer. These were derived via the pyrheliometer's calibration equation,

$$I_N = i^2 \cdot 4.27 \times 10^3 \quad (5)$$

where " i " the compensation current in ampere. The time of the pyrheliometer measurement and an ephemeris (<http://solardat.uoregon.edu/SolarPositionCalculator.html>) were used to derive the

solar zenith angle (Φ). Since the hotplate was oriented horizontally, the direct horizontal component of the irradiance appears in Equations 1, 2 and 4. The direct horizontal component was derived from values of I_N (Equation 5) and the solar zenith angle.

$$I = I_N \cdot \cos(\Phi) \quad (6)$$

All measurements were made inside an air conditioned office (temperature = 23 °C); sunlight entered the office through a south-facing window. The experiments consist of three steps: 1) the hotplate is turned on and allowed to warm up for 15 minutes while illuminated by sunlight, 2) hotplate measurements are made for 10 minutes (illuminated data) and during that time measurements were made with the pyrheliometer, and 3) the shades are drawn and hotplate measurements are made for 10 minutes (shaded data).

Table 1 presents the pyrheliometer measurements. Because the two experiments were conducted during wintertime, well before solar noon, the solar zenith angle was relatively large. Neither day had significant cloud cover, but since the path length through the atmosphere was large owing to the large zenith angle, and because of attenuation by the office window, the irradiances in the last three columns of Table 1 ($\sim 100 \text{ W m}^{-2}$) are substantially smaller than unattenuated value of the direct horizontal component ($\sim 700 \text{ W m}^{-2}$).

Figure 3 has the hotplate data from one of the two experiments. In addition to a time series of electrical power (Figure 3d), the temperature (Figure 3a), wind speed (Figure 3b), and the sensible heat (Figure 3c) time series are illustrated. The three parts of the experiment are evident with the illuminated and shaded intervals starting at 16:00 and 16:10, respectively (all times are UTC, or local time +7 hr). During the illuminated interval the temperature increases and the sensible heat decreases slightly; this behavior is expected because the rate of sensible heat transfer, as formulated in Borkhuu (2009), decreases with decreasing temperature difference

between the hotplate and its surroundings. Electrical power supplied to the hotplate (Figure 3d) is seen to shift from an average value of 9.42 W (illuminated) to 10.15 W (shaded). This increase is expected because the solar input is stopped at 16:10. Finally, the Figure 3b (hotplate windspeed) is seen to be 0 m/s for the duration of this experiment. Evidently, ventilation due to the building's heating system produced a velocity which was undetectable by the hotplate.

Table 2 summarizes the two experiments, including the direct horizontal irradiance and the time-averaged hotplate measurements from Figure 3 (electrical power and sensible heat, for both the illuminated and shaded intervals). The final column of Table 2 has the reflectance values derived using Equation 4.

Table 1 – Measurements from the pyrheliometer

Date	Time (MST)	Solar Zenith Angle (°)	Left Current (A)	Right Current (A)	Direct Normal Irradiance (Left) (W/m ²)	Direct Normal Irradiance (Right) (W/m ²)	Direct Horizontal Irradiance (Left) (W/m ²)	Direct Horizontal Irradiance (Right) (W/m ²)	Averaged Direct Horizontal Irradiance (W/m ²)
20100203	10:51	61.0	0.217	0.214	201	196	97	95	96
20100312	9:20	59.3	0.225	0.222	216	210	110	107	109

Table 2 - Measurements from the pyrheliometer and hotplate

Date	Averaged Direct Horizontal Irradiance (W/m ²)	Hotplate Electrical Power Illuminated (W)	Hotplate Electrical Power Shaded (W)	Hotplate Sensible Heat Illuminated (W)	Hotplate Sensible Heat Shaded (W)	Hotplate Reflectance
20100203	96	9.82	10.40	10.35	10.34	0.66
20100312	109	9.42	10.15	10.25	10.21	0.61

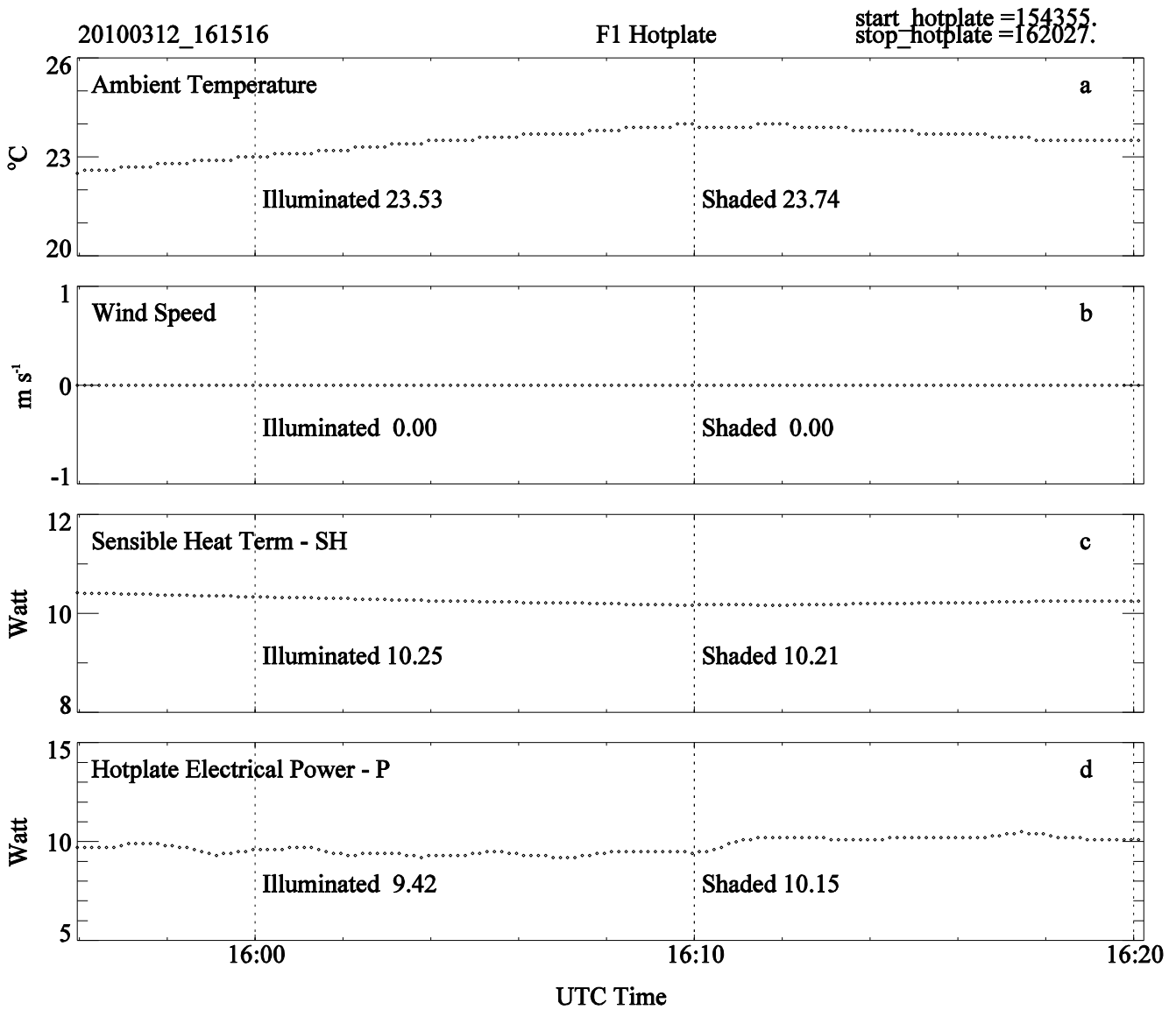


Figure 3 - (a) temperature, (b) wind speed derived from the electrical power supplied to the reference plate, temperature and wind speed, (c) sensible heat term for the sensor plate derived from temperature and wind speed via the algorithm of Borkhuu (2009), (d) electrical power supplied to the sensor plate. Measurements made on 20100312 in an office in the College of Engineering and Applied Science at the University of Wyoming. Data is acquired at 1 Hz. Plotted values are resampled at 0.1 Hz.

Discussion and Conclusion:

We report two experimental determinations of the fraction of solar energy reflected by the upward-oriented surface of the Yankee Environmental Systems Hotplate Precipitation Sensor. Our two determinations of the reflectance are 0.66 and 0.61 and their average is 0.63. This average is slightly smaller than the value reported for polished aluminum reflecting “incandescent” light (0.69; Weast, 1975) and significantly smaller than the value for vacuum-deposited aluminum at visible wavelengths (0.97; Hass, 1955). As can be seen from Figure 1 the hotplate surface is not polished. Furthermore, since the reflectance of vacuum-deposited metal is significantly larger than that of a polished metal surface (Hass, 1955), our reflectance determination is qualitatively consistent and perhaps even quantitatively consistent with values reported in the literature. Repeated assessment of the reflectance is needed to specify the precision of the measurement. An uncertainty analysis, and comparison of the irradiance measurement to a reference standard, are needed to gauge the absolute accuracy of the reflectance.

References

- Borkhuu, B., Snowfall at a High Elevation Site: Comparisons of Six Measurement Techniques, M.S. Thesis, Department of Atmospheric Science, University of Wyoming, 2009
- Epply Laboratory., The Epply-Angstrom Compensation Pyrheliometer and Associated D.C. Electrical Instrumentation, 1976
- Hass, G., Filmed surfaces for reflecting optics, Journal of the Optical Society of America, 945-952, 1955
- King, W.D., D.A.Parkin, R.J.Handsworth, A hot-wire liquid water device having fully calculable response characteristics, J. Appl. Meteor., 17, 1809-1813, 1978
- Korolev, A.V., J.W.Strapp, G.A.Isaac, A.N.Nevzorov, The Nevzorov airborne hot-wire LWC-TWC probe: Principle of operation and performance characteristics, J. Atmos. Oceanic Tech., 15, 1495-1510, 1998
- Rasmussen, R., Hallett, J., Purcell, R., Landolt, S.D., Cole, J., The hotplate snow gauge, Submitted to Journal of Applied Meteorology and Climatology, 2010
- Weast, R.C., Ed., Handbook of Chemistry and Physics, 56th ed, Chemical Rubber Company, Cleveland, Ohio, 1975
- Wolfe, J.P., and J.R.Snider, A reflectivity/snowrate relationship for S-band radar at a high-altitude Site, submitted to Journal of Applied Meteorology and Climatology, 2010